7

Chapter 7

Unsteady Elastico-viscous Boundary Layer Stagnation-point Slip Flow and Heat Transition along a Stretching Surface

7.1 Introduction

The practical significance lies in the fluid movement and heat transfer that occurs along a stretching surface. Such flows are ubiquitous in technological and industrial processes, and the final product's quality is significantly affected by the cooling pace. As a result, heat transport should be managed to produce a superior product. In fluid mechanics, the boundary layer flow is extremely important since the entire dynamic is triggered by the boundary surface. The boundary layer theory is essential for modelling various types of fluids and hence, for solving derived equations utilising similarity variables.

A significant number of crucial industrial fluids exhibit non-Newtonian characteristics. Such fluids are now widely accepted as being more appropriate in real-world industrial applications than Newtonian fluids. The non-Newtonian viscoelastic fluid displays viscous and elastic characteristics. When pressure is applied to it with high velocity, it hardens and changes its state from liquid to solid, and thus it is widely used in protective equipment. The non-Newtonian flow generated by a stretching sheet has several uses in a wide variety of industries and manufacturing processes. Examples include paper,

fibre and plastic sheet production, food processing, metal spinning, hot rolling, wire coating, etc.

When a solid object is in the path of the flow and there is zero velocity at that point, the flow becomes stagnant. This flow pattern is commonly used in dental procedures and air filtration systems. The fluctuation in temperature and flow rate of a viscous fluid close to its stagnation point was investigated by Mahapatra *et al.* [122] over a stretched sheet. Nazar *et al.* [123] explored the time-varying fluid flow around the stagnation point across a deforming surface. Hayat *et al.* [124] used MHD to analyze the micropolar fluid dynamics across a nonlinear stretching sheet. Mukhopadhyay and Swati [125] demonstrated the heat transition process of an unstable free and force convection flow along a vertically expanding surface.

The unsteady flow condition is often noticed when the flow is reliant on time in many circumstances. Ishak *et al*. [126] examined the nature of quiescent fluid along a stretching surface. The partial slip impact on the flow field close to stagnation point past a contracting surface was studied by Bhattacharyya *et al.* [127]. Bhattacharyya [128] also demonstrated Casson fluid flow adjacent to stagnation point, as well as heat transfer in the direction of a contracting or expanding sheet. Khalid *et al*. [129], Seth et al. [130], Dzulkifli *et al.* [131], Rosali *et al.* [132] also examined the flow and heat transmission processes adjacent to the stagnation point, considering different flow properties.

Layek *et al.* [133] presented the heat transfer and flow symmetry for non-Newtonian fluids considering power-law fluid with thermal radiation across a nonlinearly contracting/expanding sheet. The impact of slip on fluid mass transportation and heat transport process in an MHD unsteady flow on a stretched surface were studied numerically by Mabood *et al.* [134]. Alghamdi *et al.* [135] investigated the attributes of nanofluid hybrid flow over a stretched surface as it nears a stagnation point. Agrawal *et al.* [136] examined the fluid motion and heat transport of MHD non-linear porous stretching sheet considering slip factors. Mabood *et al.* [137] presented the visco-elastic nature of nanofluid along a stretching cylinder. Debnath and Saha [138, 139,140,141] examined the flow behaviour of elastic-viscous fluid considering different geometry. Saha and Debnatht [142] investigated the reactive solute diffusion in elastic-viscous fluid past a flat porous plate.

The fluid motion and heat transport across a stretching surface in an unsteady elastico-viscous boundary layer with Walters Liquid (Model $\boldsymbol{B}'$) is investigated in this study.

7.2 Mathematical Formulation

The heat transition for unsteady elastico-viscous fluid flow close to the stagnation point is examined for a stretching surface with velocity $U_w(x,t)$. The temperature $T_w\ (x,t)$ of the stretching surface changes with time and distance in the x-direction of the sheet. The following set of eqs. regulate the fluid motion:

$$u_x + v_y = 0 \tag{7.2.1}$$

$$u_t + uu_x + vu_y = -\frac{1}{\rho}p_x + \nu u_{yy} - \mathrm{k}_0(\rho)^{-1}\left(u_{tyy} + uu_{xyy} + vu_{yyy} - u_y u_{xy} - v_y u_{yy}\right) \tag{7.2.2}$$

$$T_t + uT_x + vT_y = K\left(\rho C_p\right)^{-1} T_{yy} \tag{7.2.3}$$

where, u: velocity in the x-directions, v: velocity in the y-directions and other symbols have their usual meaning.

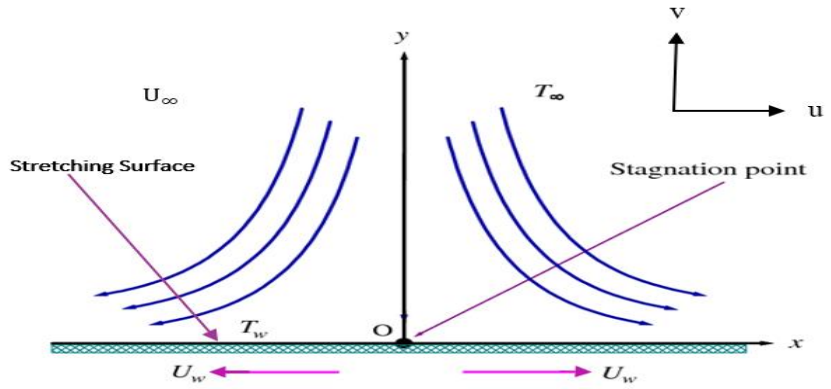

Fig. 7.1: Physical sketch of flow model

In the inviscid free stream, $u = U_\infty(x,t)$, hence from (6.2.2) one can write

$$(\mathrm{U}_\infty)_t + \mathrm{U}_\infty(\mathrm{U}_\infty)_x = -(\rho)^{-1}p_x \tag{7.2.4}$$

where, U_∞ is the stagnation flow velocity in a free stream.

Hence, (7.2.2) becomes

$$u_t + uu_x + vu_y = (\mathrm{U}_\infty)_t + \mathrm{U}_\infty(\mathrm{U}_\infty)_x + \nu u_{yy} - \frac{\mathrm{k}_0}{\rho}\left(u_{tyy} + uu_{xyy} + vu_{yyy} - u_y u_{xy} - v_y u_{yy}\right) \tag{7.2.5}$$

The relevant boundary conditions

$$u = U_w(x,t) + N_1 \upsilon u_y, v = 0 \text{ at } y = 0; \quad u \to U_\infty(x,t) \text{ as } y \to \infty \tag{7.2.6}$$

$$T = T_w + D_1 T_y \text{ at } y = 0; \quad T \to T_\infty \text{ as } y \to \infty \tag{7.2.7}$$

The suitable form of stretching and stagnation velocities are $U_w(x,t) = cx(1-\alpha t)^{-1}$ and $U_\infty(x,t) = ax(1-\alpha t)^{-1}$, where $c(>0)$: stretching parameter, $\alpha(>0)$: a constant, $a(>0)$: straining parameter, $N_1(=N\sqrt{1-\alpha t})$: velocity slip factor, $D_1(=D\sqrt{1-\alpha t})$: thermal slip factor, N: initial velocity slip factor, D: initial thermal slip factor.

Surface temperature $T_w\ (x,t)$ is chosen as

$$T_w = T_\infty + T_0(cx^2)(2\upsilon)^{-1}(1-\alpha t)^{-\frac{3}{2}} \tag{7.2.8}$$

where, T_∞: constant temperature of free stream, T_0: constant determining rate of surface temperature.

Similarity variables are taken as:

$$\psi = \left(\frac{c\upsilon}{1-\alpha t}\right)^{\frac{1}{2}} x f(\eta), T = T_\infty + (T_w - T_\infty)\theta(\eta) \text{ and } \eta = y\left(\frac{c}{\upsilon(1-\alpha t)}\right)^{\frac{1}{2}} \tag{7.2.9}$$

with $u = \psi_y$ and $v = -\psi_x$, where ψ: stream function and η: similarity variable.

In view of (7.2.9), equation (7.2.5) and (7.2.3) take the form

$$f''' + ff'' - (f')^2 - A\left(f' + \frac{\eta}{2}f'' - \frac{a}{c}\right) + \left(\frac{a}{c}\right)^2 - k_1\left[A\frac{\eta}{2}f^{iv} + 2Af''' - ff^{iv} + 2f'f''' - (f'')^2\right] = 0 \tag{7.2.10}$$

$$\theta'' + Pr\left(f\theta' - 2f'\theta - \frac{A}{2}(3\theta + \eta\theta')\right) = 0 \tag{7.2.11}$$

where $\frac{a}{c}$ and $A = \frac{\alpha}{c}$ represent velocity and unsteadiness parameter respectively, $Pr = \frac{\mu c_p}{k}$: Prandtl number.

Reduced conditions at the boundary are

$$f(\eta) = 0,\ f'(\eta) = 1 + \lambda f''(\eta)\ at\ \eta = 0\ ; f'(\eta) = \frac{a}{c},\ f''(\eta) = 0\ as\ \eta \to \infty \tag{7.2.12}$$

$$\theta(\eta) = 1 + \delta\theta'(\eta)\ at\ \eta = 0\ ;\ \theta(\eta) \to 0\ as\ \eta \to \infty \tag{7.2.13}$$

where $\lambda = N\sqrt{cv}$: transformed velocity slip parameter and $\delta = D\sqrt{\frac{c}{v}}$: transformed thermal slip parameter.

7.3 Method of Solution

To employ Matlab inbuilt solver bvp4c, (7.2.10) and (7.2.11) are reduced as

$$f = y_1, f' = y_2,\ f'' = y_3, f''' = y_4\ , \theta = y_5, \theta' = y_6 \tag{7.3.1}$$

From (7.3.1), we can write as

$$y_1' = y_2, y_2' = y_3, y_3' = y_4, y_5' = y_6 \tag{7.3.2}$$

Making use of (7.3.1) and (7.3.2), the equations (7.2.10) and (7.2.11) can be written as

$$y_4^{/} = \frac{1}{\left(A\frac{\eta}{2} - y_1\right)}\left[y_3^2 - 2y_2y_4 - 2Ay_4 - \frac{1}{k_1}\left\{y_4 + y_1y_3 - y_2^2 - A\left(y_2 + \frac{\eta}{2}y_3 - \frac{a}{c}\right) + \left(\frac{a}{c}\right)^2\right\}\right] \tag{7.3.3}$$

$$y_6^{/} = -\Pr\left\{y_1y_6 - 2y_2y_5 - \frac{A}{2}(3y_5 + \eta y_6)\right\} \tag{7.3.4}$$

and the relevant boundary conditions (7.2.12) and (7.2.13) reduces as follows:

$$y_1(0) = 0, y_2(0) = 1+\lambda y_3(0)\ and\ \ y_2(\infty) = \frac{a}{c}, y_3(\infty) = 0 \tag{7.3.5}$$

$$y_5(0) = 1 + \delta y_6(0)\ and\ \ y_5(\infty) = 0 \tag{7.3.6}$$

The above equations are considered to write down the programming codes and plotting velocity and temperature curves with the help of involved flow feature parameters.

7.4 Results and Discussion

The built-in MATLAB programme 'bvp4c' is used to plot velocity and temperature curves, emphasizing the importance of the flow pattern in terms of its physical significance for the flow parameters involved in the flow field. Figs. 7.2 to 7.14 are the visual depictions of involved flow parameters' effects on the findings. To verify the correctness of current work, the numerically computed values produced using the Matlab solver ‘bvp4c’, skin friction coefficient $f''(0)$ are evaluated. The acquired results agree with the standard values that have previously been published, as presented in Table 7.1.

Table 7.1 Values of $f''(0)$ for different values of $\frac{a}{c}$ with $A = k_1 = \lambda = \delta = 0$

$\frac{a}{c}$	Mahapatra and Gupta [103]	Nazar et al. [104]	Bhattacharyya et al. [108]	Present study
0.1	-0.9694	-0.9694	-0.9694	-0.9694
0.2	-0.9181	-0.9181	-0.9181	-0.9181
0.5	-0.6673	-0.6673	-0.6673	-0.6673
2.0	2.0175	2.0175	2.0175	2.0175
3.0	4.7293	4.7296	4.7293	4.7292

Fig. 7.2 depicts the velocity curves $f'(\eta)$ against η for variation of $\frac{a}{c}$ under (a) slip and (b) no-slip boundary conditions. For $\frac{a}{c} > 1$, boundary layer thickness diminishes with the growth of $\frac{a}{c}$ and, similarly, for $\frac{a}{c} < 1$, it reduces with growing $\frac{a}{c}$. But, for $\frac{a}{c}$ = 1, no boundary layer structure is noticed, which signifies the physical behavior of the fluid.

Velocity curves $f'(\eta)$ against η for varations of k_1 under (a) slip and (b) no-slip boundary conditions for $\frac{a}{c}$ = 1.5 & $\frac{a}{c}$ = 0.5 are presented in Figs.7.3 and 7.4. Fig.7.3 indicates that the velocity enhances initially but with the rise of k_1, the fluid motion diminishes for both the cases. Whereas the reverse pattern is observed in Fig. 7.4, it shows that $\frac{a}{c}$ plays an important role for increasing and decreasing velocity in the flow field.

Figs. 7.5 and 7.6 demonstrate the velocity curves $f'(\eta)$ against η for variaton of A with (a) slip and (b) no-slip boundary conditions for $\frac{a}{c}$ = 1.5 & $\frac{a}{c}$ = 0.5. When A is raised, the velocity at a point rises, causing the boundary layer's thickness to fall for $\frac{a}{c} = 1.5$ but thickness of boundary layer grows with the rise of A with slip and non-slip conditions, despite the fact that starting velocity at a location decreases.

Velocity curves $f'(\eta)$ against η for variation of λ with (a) slip and (b) no-slip boundary conditions for $\frac{a}{c}$ = 1.5 & $\frac{a}{c}$ = 0.5 are portrayed in fig. 7.7. It is noticed that for both $\frac{a}{c}$ values, the velocity boundary layer thins down quickly as λ rises.

Fig. 7.8 depicts temperature curves $\theta(\eta)$ against η for two different boundary conditions: (a) slip and (b) no-slip for distinct values of $\frac{a}{c}$. When a/c increases, $\theta(\eta)$ reduces

noticeably for fixed η, and thus thermal boundary layer becomes thin. The thermal boundary layer is also seen for a/c = 1.

Temperature profiles $\theta(\eta)$ versus η for distinct values of k_1 at the boundary: (a) slip and (b) no-slip for a/c = 1.5 and a/c = 0.5 are presented in Figs. 7.9 and 7.10. Fig. 7.9 shows that the temperature curves decrease at first, then rise somewhat with rising values of k_1, yet Fig. 7.10 shows the opposite pattern. The fluid temperature is significantly influenced by the velocity ratio parameter a/c.

Figs. 7.11 and 7.12 show temperature curves $\theta(\eta)$ against η for variation of A, with (a) a slip and (b) no slip boundary conditions. The fluid temperature reduces at all points with the rise of A for distinct values of a/c with slip and no-slip conditions.

Temperature curves $\theta(\eta)$ against η for distinct values of λ are shown in Fig. 7.13, with (a) slip and (b) no-slip boundary conditions for a/c = 1.5 and a/c = 0.5. At a given point, the temperature reduces when a/c approaches 1.5, but it rises sharply as a/c approaches 0.5.

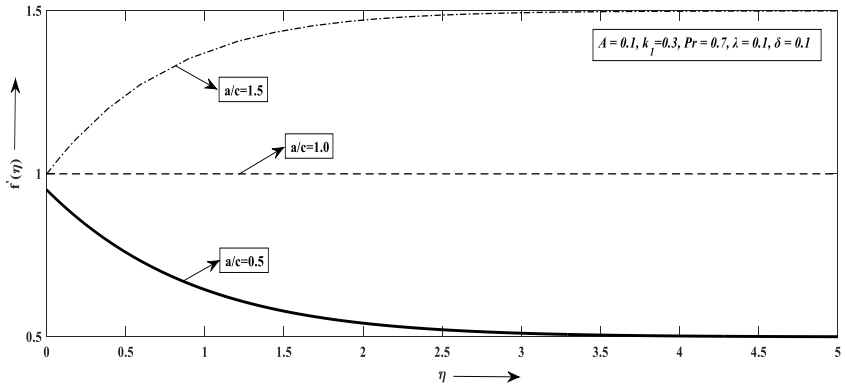

Fig.7. 2 (a) Plot of $f'(\eta)$ for variation of a/c taking $\lambda \neq 0$

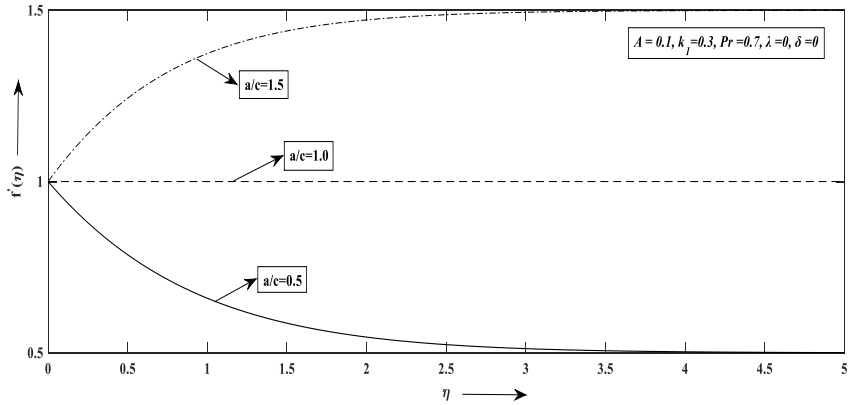

Fig.7. 2 (b) Plot of $f'(\eta)$ for variation of a/c taking $\lambda = 0$

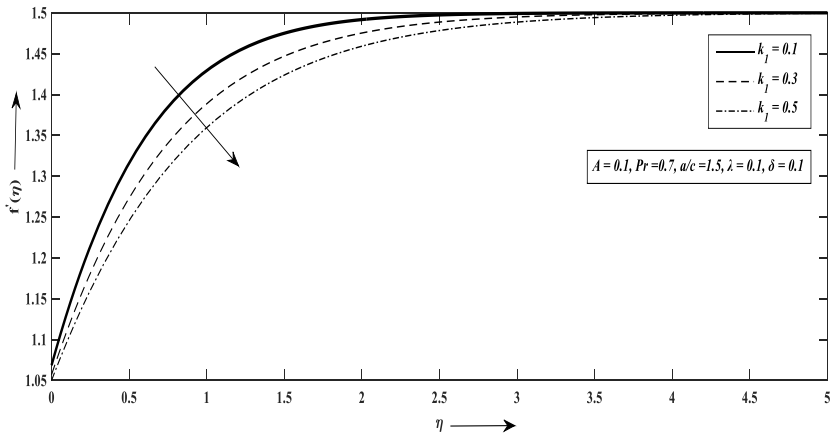

Fig. 7.3 (a) Plot of $f'(\eta)$ for variation of k_1 taking $\lambda \neq 0$ for a/c =1.5

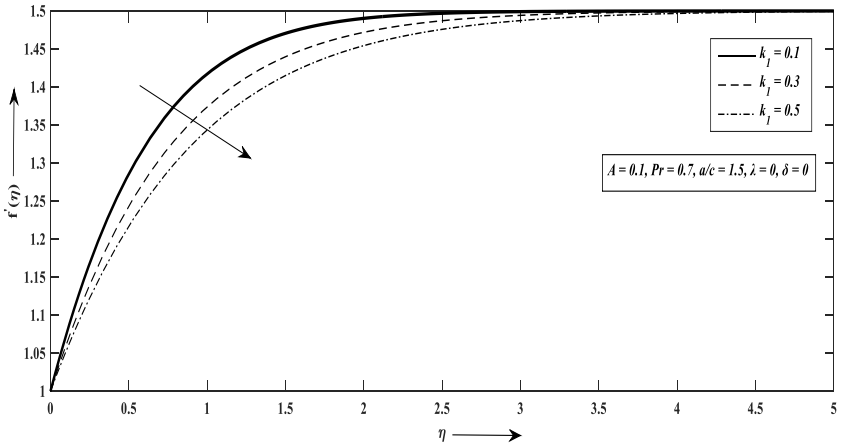

Fig. 7.3 (b) Plot of $f'(\eta)$ for variation of k_1 taking $\lambda = 0$ for a/c =1.5

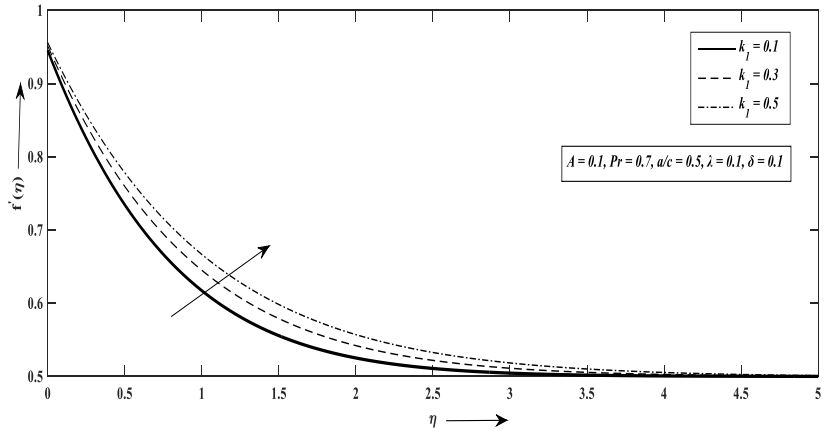

Fig. 7.4 (a) Plot of $f'(\eta)$ for variation of k_1 taking $\lambda \neq 0$ for a/c =0.5

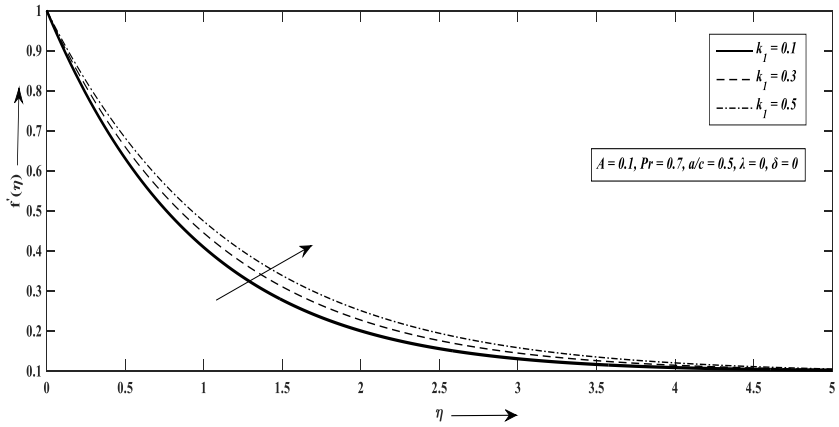

Fig. 7.4 (b) Plot of $f'(\eta)$ for variation of k_1 taking $\lambda = 0$ for a/c =0.5

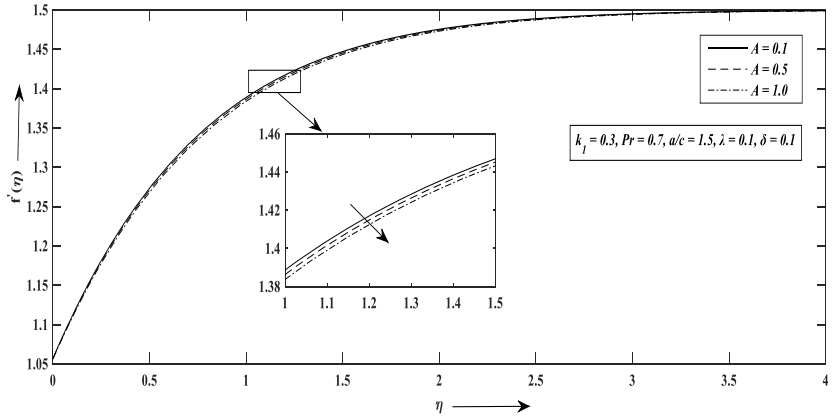

Fig. 7.5 (a) Plot of $f'(\eta)$ for variation of A taking $\lambda \neq 0$ for a/c =1.5

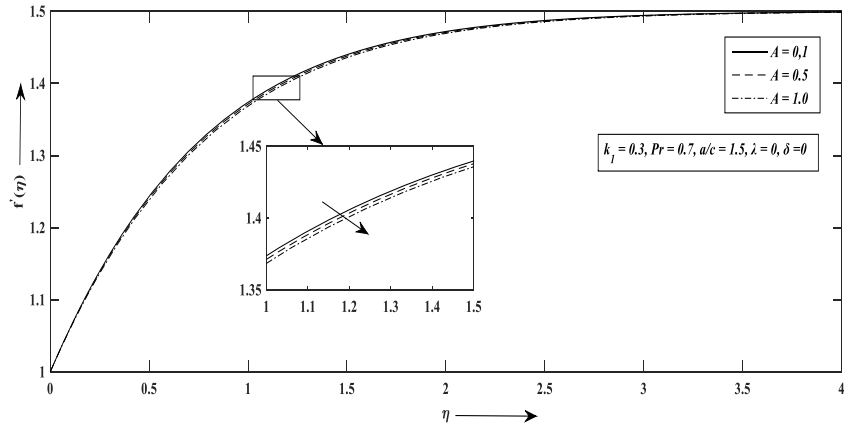

Fig. 7.5 (b) Plot of $f'(\eta)$ for variation of A taking $\lambda = 0$ for a/c =1.5

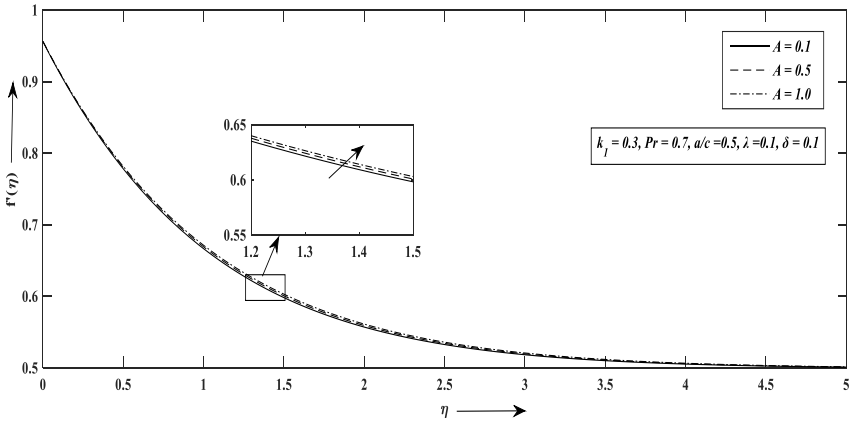

Fig. 7.6 (a) Plot of $f'(\eta)$ for variation of A taking $\lambda \neq 0$ for a/c =0.5

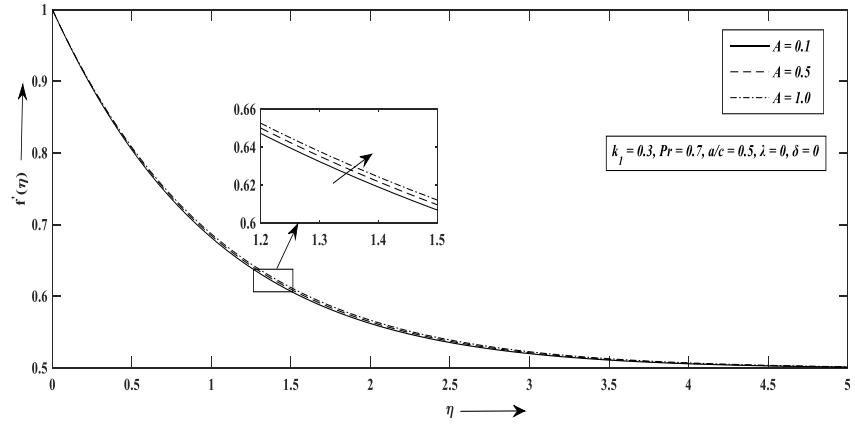

Fig. 7.6 (b) Plot of $f'(\eta)$ for variation of A taking $\lambda = 0$ for a/c =0.5

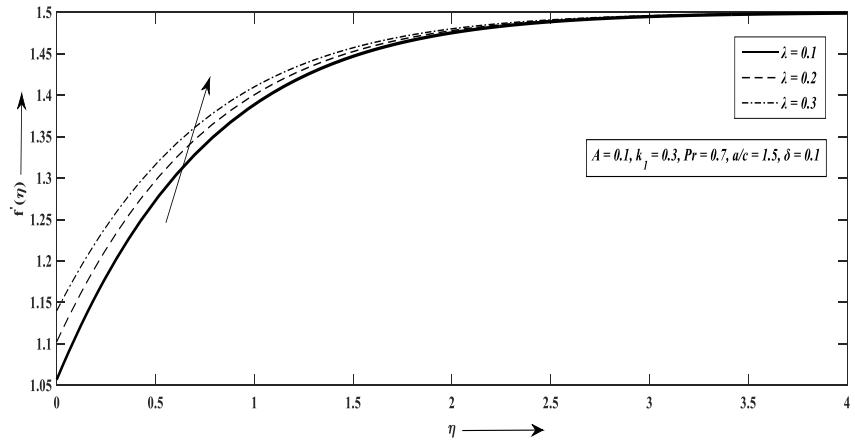

Fig. 7.7 (a) Plot of $f'(\eta)$ for variation of λ for a/c =1.5

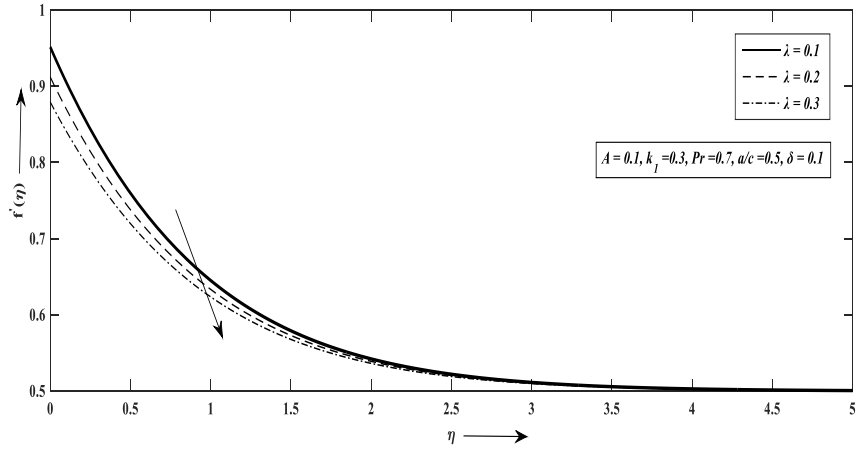

Fig. 7.7 (b) Plot of $f'(\eta)$ for variation of λ for a/c =0.5

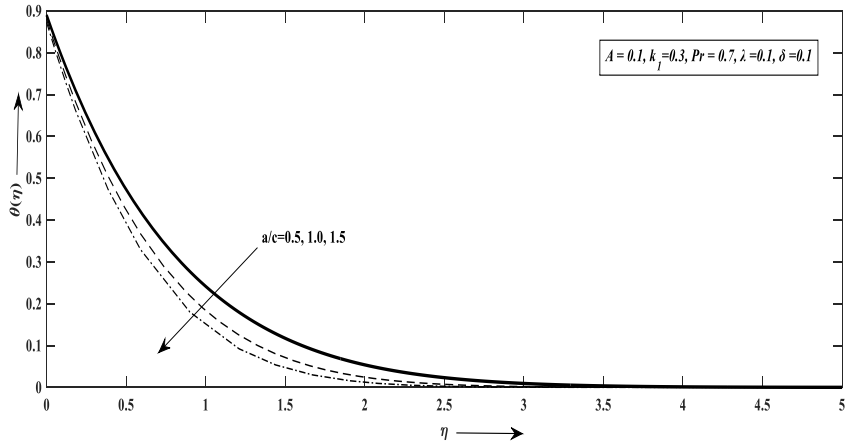

Fig. 7.8 (a) Plot of $\theta(\eta)$ for variation of a/c taking $\delta \neq 0$

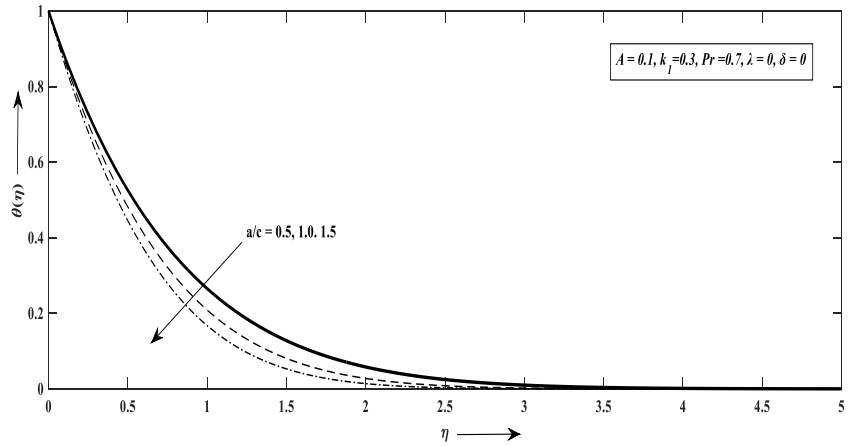

Fig.7.8 (b) Plot of $\theta(\eta)$ for variation of a/c taking $\delta = 0$

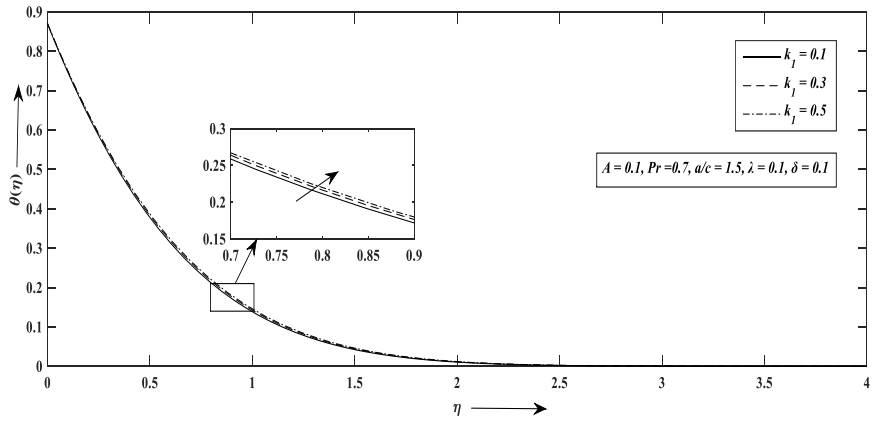

Fig.7.9 (a) Plot of $\theta(\eta)$ for variation of k_1 taking $\delta \neq 0$ for a/c =1.

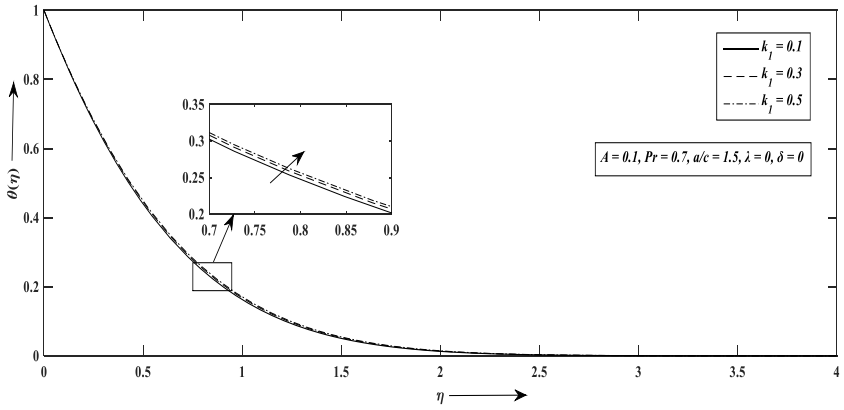

Fig.7.9 (b) Plot of $\theta(\eta)$ for variation of k_1 taking $\delta = 0$ for a/c =1.5

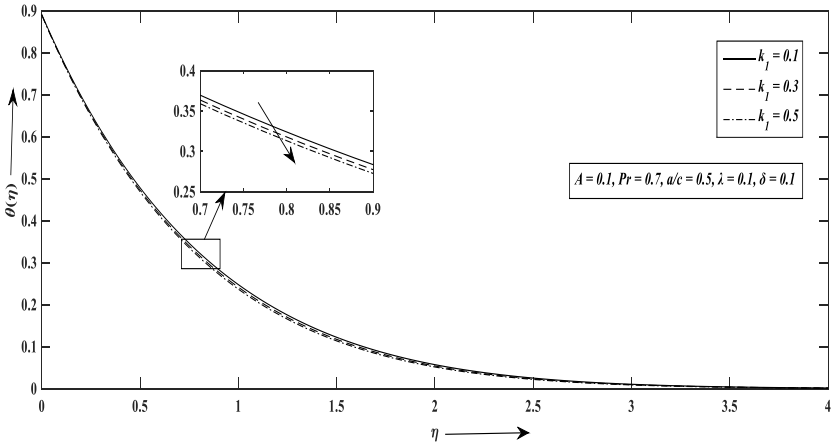

Fig. 7.10 (a) Plot of $\theta(\eta)$ for variation of k_1 taking (a) $\delta \neq 0$ for a/c =0.5

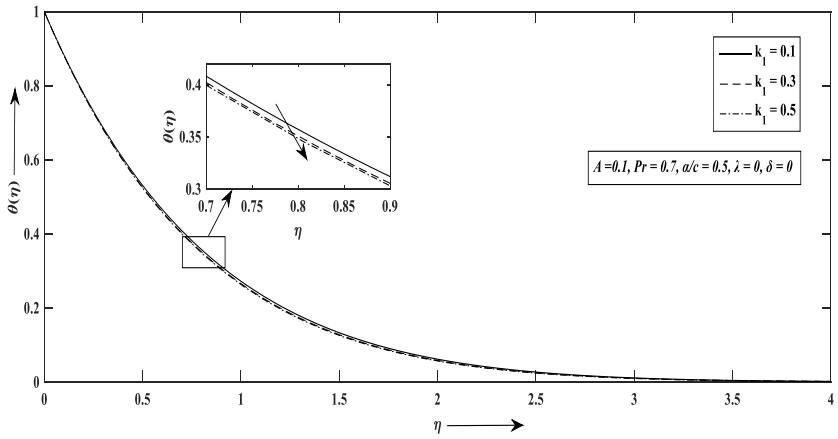

Fig. 7.10 (b) Plot of $\theta(\eta)$ for variation of k_1 taking $\delta = 0$ for a/c =0.5

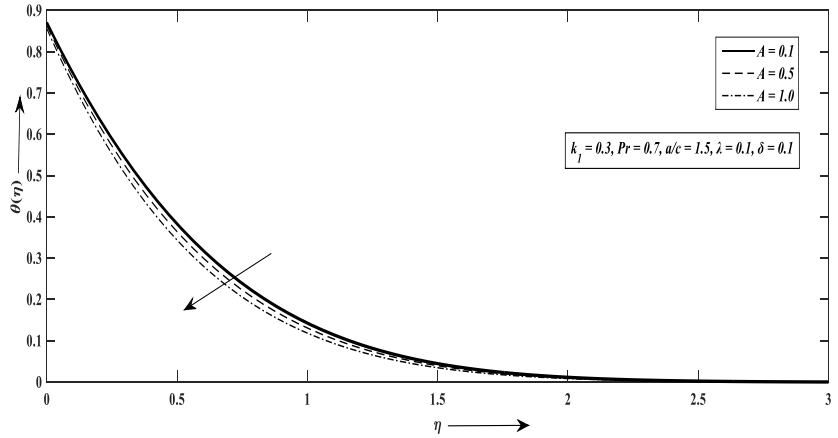

Fig.7.11(a) Plot of $\theta(\eta)$ for variation of A taking $\delta \neq 0$ for a/c =1.5

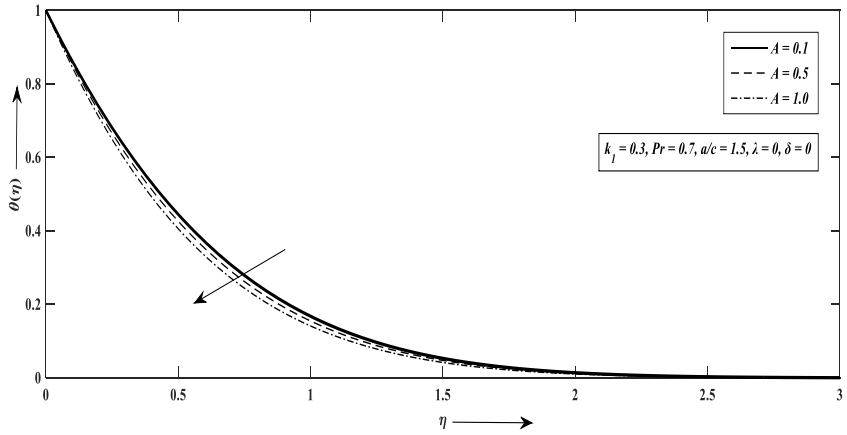

Fig.7.11(b) Plot of $\theta(\eta)$ for variation of A taking $\delta = 0$ for a/c =1.5

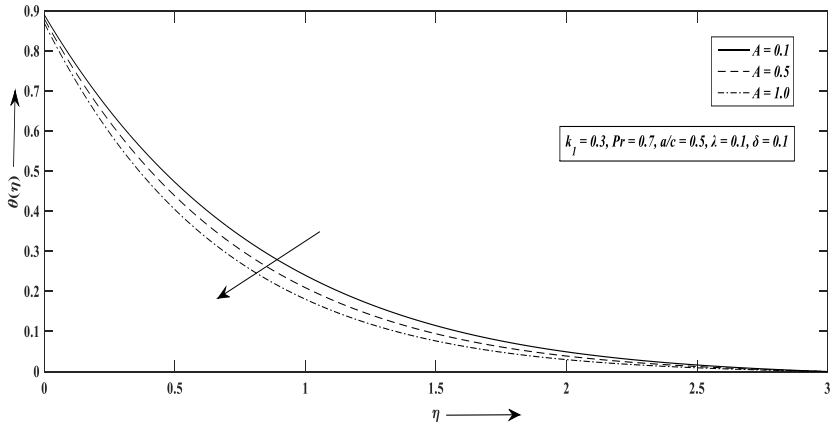

Fig. 7.12 (a) Plot of $\theta(\eta)$ for variation of A taking $\delta \neq 0$ for a/c =0.5

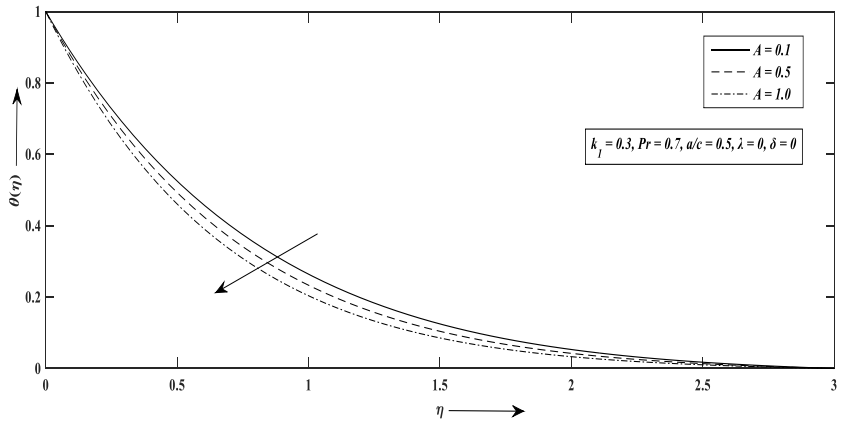

Fig. 7.12 (b) Plot of $\theta(\eta)$ for variation of A taking $\delta = 0$ for a/c =0.5

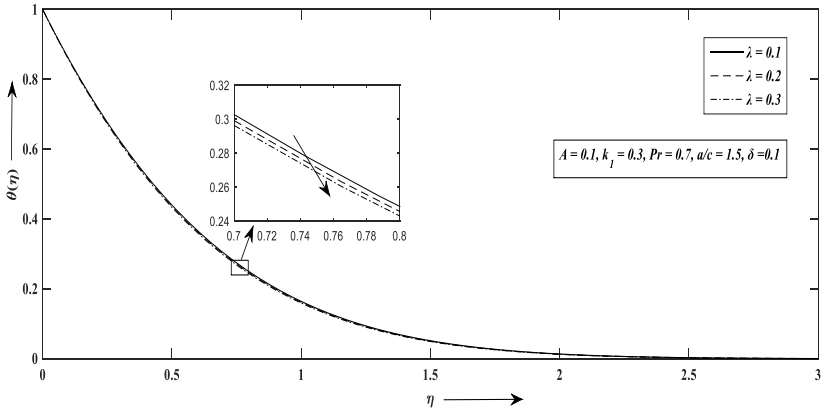

Fig. 7.13 (a) Plot of $\theta(\eta)$ for variation of λ for (a) a/c =1.5

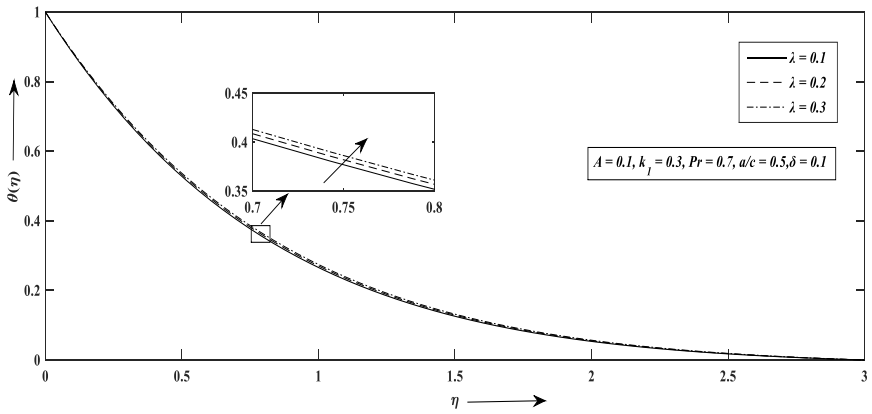

Fig. 7.13 (b) Plot of $\theta(\eta)$ for variation of λ for a/c =0.5

7.5 Conclusions

The following conclusion can be drawn from this paper:

- Elastico-viscous and velocity ratio factors have a substantial effect on fluid motion.
- Fluid motion and heat transition can be controlled by adjusting velocity and thermal slip factors.
- Transition of thermal energy reduces for rising values of almost all the flow parameters.
- The unsteadiness constant plays a role in enhancing the rate of thermal transition of the fluid.
- Velocity ratio parameter heavily influenced the fluid dynamics.
- Slip factors help to control the boundary layer thickness under slip and no-slip conditions.
- Boundary layer thickness can be controlled by the slip parameters.

Scope for future work

The future scope of research on viscoelastic fluid flow is vast and holds great potential for advancements in various fields such as fluid dynamics, material science, biology, and engineering. It is crucial to develop accurate and efficient mathematical models to characterize the behaviour of viscoelastic fluids. Microfluidic devices are widely used in various applications, and understanding the behaviour of viscoelastic fluids at the microscale is essential for their efficient operation. Viscoelastic fluids have significant industrial applications, such as in polymer processing, food processing, and oil drilling. Future research can explore ways to optimize manufacturing processes, design better mixing and pumping systems, and develop advanced materials with tailored rheological properties. Viscoelastic fluids play a crucial role in various biological systems, such as blood flow, mucus transport, and cell mechanics. Studying the behaviour of these fluids in biological contexts can provide insights into disease mechanisms and lead to the development of new diagnostic and therapeutic approaches. Viscoelastic fluids can exhibit unique properties, such as shear-thinning or shear-thickening behaviour, which can be harnessed for the development of smart materials and devices such as soft robotics, flexible electronics, bullet proof jackets, speed bump, etc. Advancements in this field has the potential to improve understanding of complex fluid behaviour and pave the way for innovative technologies with improved performance and efficiency.

Due to diversified applications displayed by the problems discussed in this thesis, it may be remarked that there is enough scope of doing further research in this field. Some fluid properties have been discussed in this study but there are many rheological properties of fluids of engineering interest which may be incorporated for further research. It is also possible to conduct a comparative analysis of different numerical and analytical methods for solving the same problem. Additionally, a future study that focuses on flow simulation and stability analysis of the problem would be highly intriguing. As per requirement of the fluid flow situation different suitable geometrical configurations and coordinate systems may be considered. It is possible to employ Lie group and Homotopy analysis method to develop the constitutive model. The results of this investigation will act as a source of inspiration for future experimental work, which appears to be missing at the moment.